

Experimental study on infilled frames strengthened by profiled steel sheet bracing

Pingzhou Cao^{*}, Ningning Feng^a and Kai Wu^b

College of Civil and Transportation Engineering, Hohai University, Nanjing, Jiangsu, P.R. China

(Received January 15, 2014, Revised March 03, 2014, Accepted April 28, 2014)

Abstract. The purpose of this study is to investigate the seismic performance of reinforced concrete (RC) frames strengthened by profiled steel sheet bracing which takes the influence of infill walls into consideration. One-bay, two-story, 1/3 scale two specimens shared same feature of dimensions, one specimen consists only beams and columns; the other one is reinforced by profiled steel sheet bracing with infill walls. Hysteretic curves, envelope curves, stiffness degradation curves and energy dissipation capacities are presented based on test data. Test results indicate that the ultimate load of strengthened specimen has been improved by 225%. The stiffness of reinforced by profiled steel sheet bracing has been increased by 108%. This demonstrates that infill walls and profiled steel sheet bracing enhanced the strength and stiffness distinctly. Energy dissipation has an obvious increase after 12 cycles. This shows that the reinforced specimen is able to bear the lateral load effectively and absorb lots of seismic energy.

Keywords: reinforced concrete frames; infill walls; profiled steel sheet bracing; seismic performance; cyclic load

1. Introduction

In view of the damage of RC frame structure in the earthquake, it is necessary to reinforce the existing reinforced concrete buildings which are lack of lateral stiffness and seismic behavior. According to the damage of RC frames, carbon fiber (Altin *et al.* 2008, Erdem *et al.* 2006, Guo and Zhao 2012, Zhu *et al.* 2011) and steel bracing (Bush *et al.* 1991, Badoux and Jirsa 1990, Wang *et al.* 1998) reinforcement are common methods to reinforce frames. Maheri and Hadjipour (2003) analyzed three types of brace/RC frame connections. One was X-bracing, which connected to beam-column joints. The other one was also X-bracing, which connected to the steel plates. The third one made X-bracing fix to a special connection, which transferred the brace load directly through the joint. Test results indicated that X-bracing corresponded well with RC frames. Fell *et al.* (2009) adopted steel bracing to reinforce RC frame. The results showed that the frame has enhanced the strength and stiffness. The ultimate bearing capacity depended on brace buckling, the damage of connector and shear failure of column. Zhao *et al.* (2013) researched one-bay two-story

*Corresponding author, Professor, E-mail: pzcao@hhu.edu.cn

^a Ph.D. Student, E-mail: fengningning1104@163.com

^b Ph.D., E-mail: wukai19811240@163.com

RC frame, which reinforced by Y-eccentrically steel bracing. Experimental results showed that the use of Y-eccentrically steel bracing was rational and feasible. Yu (2009) discussed the seismic performance of welded I-section steel bracing members. One-twelfth steel frame was strengthened by this steel bracing. Test results showed that it was reasonable to use the steel bracing in 8 degree (seismic intensity) areas.

On the basis of these studies, it is seldom research that profiled steel sheet bracing reinforces RC frames experimentally. Therefore, in virtue of the quality of light, low cost and tensile property, profiled steel sheet bracing is used to reinforce RC frames in this paper. In general, profiled steel sheeting is widely used in composite floors (Nie and Yi 2005 and Li *et al.* 2008). Tzaros *et al.* (2010) have introduced bending tests on composite slabs with profiled steel sheeting. Nonmonotone law was used in dealing with the shear bonding between the concrete and the profiled steel sheeting. The analysis revealed that numerical results were consistent with the experimental results. Ahmed and Badaruzzaman (2013) have studied Profiled Steel Sheet Dry Board (PSSDB) composite panel. A study of vibration test has been carried out on different thickness and different space of connector. Furthermore, numerical simulation was conducted by the commercially available finite element code LUSAS. It was found that 16-24 mm thick board and 100-200 mm spacing of connector were suitable for PSSDB composite panel. Chen (2002) have used 3 groups of steel deck-concrete composite slabs to research the load-carrying capacities and flexural behavior. According to the test results, the computational formula about the longitudinal shear-bond strength has been proposed.

The test consists of two specimens. Specimen KJ-1 is bare without infill walls and profiled steel sheet bracing. Specimen KJ-2 adds profiled steel sheet bracing and infill walls. The objective of the present study is to investigate seismic performance of Specimen KJ-2 by the experimental model test. The evaluation method basing on the comparison of hysteretic curves, envelope curves, stiffness degradation curves and energy dissipation capacities are discussed.

2. Experimental program

2.1 Specimen design

Two specimens of KJ-1 and KJ-2 were designed and constructed with same dimensions and steel skeletons as shown in Fig. 1, which were both tested under low cyclic reversed loading. The clear span was 1.8 m, story height was 1.2 m and the total height was 3.4 m. The cross sections of beam and column were 120×200 mm and 200×200 mm, respectively.

Considering the connection between frame and profiled steel sheeting, there were three steps in the process. The first step was to install steel plates $200 (280) \times 35 \times 4$ mm to beams and columns. Steel plates were located on the left and right of columns, and on the up and down of beams. Every two steel plates were connected by two steel rods. The second step was to weld channel steel $100 \times 100 \times 2$ mm onto steel plates, masonrying wall in the channel steel. At last, tapping screws were used to connect profiled steel sheeting and channel steel. Profiled steel sheet bracing located in both sides of the wall and showed X shape. The layouts of infill walls and profiled steel sheet bracing are shown in Fig. 2. Fig. 3 is the photograph of the layouts of Specimens KJ-2.

As a new type of strengthening technique, the study of profiled steel sheet bracing reinforced method is at the stage of experimentation at present. When this strengthening technique is applied to the existing RC frames, hammer anchor will replace steel plates and steel rods. Hammer anchor

is an expansion bolt, which connects the frame and profiled steel sheeting conveniently. Profiled steel sheeting is fixed on one side of beams to avoid making holes in the floor and infill walls.

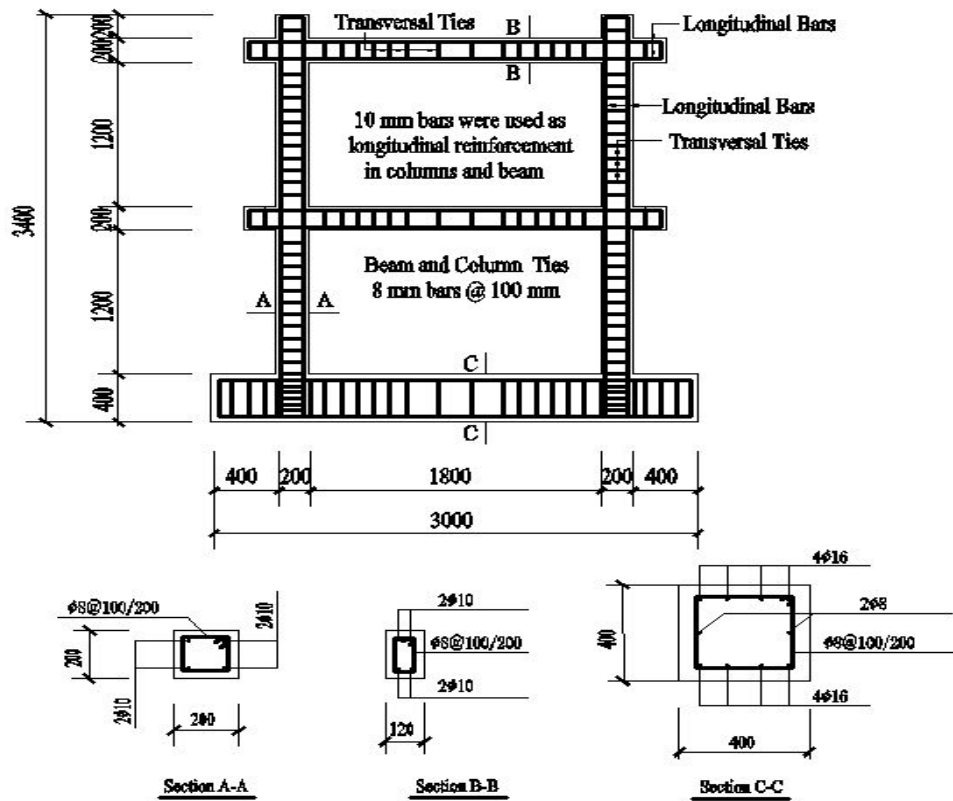


Fig. 1 Design details for test specimens

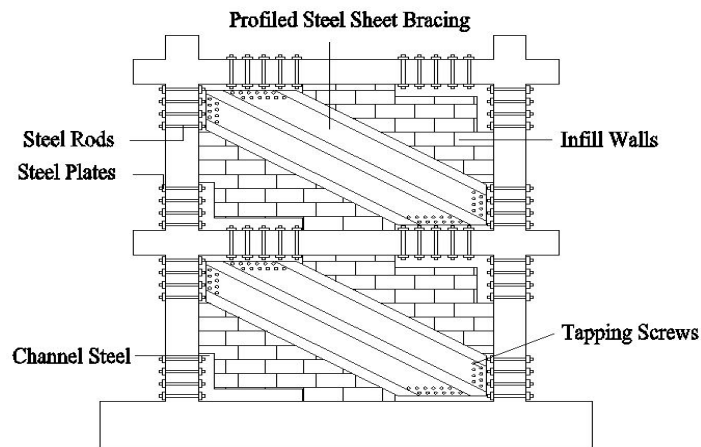


Fig. 2 Layouts of infill walls and profiled steel sheet bracing

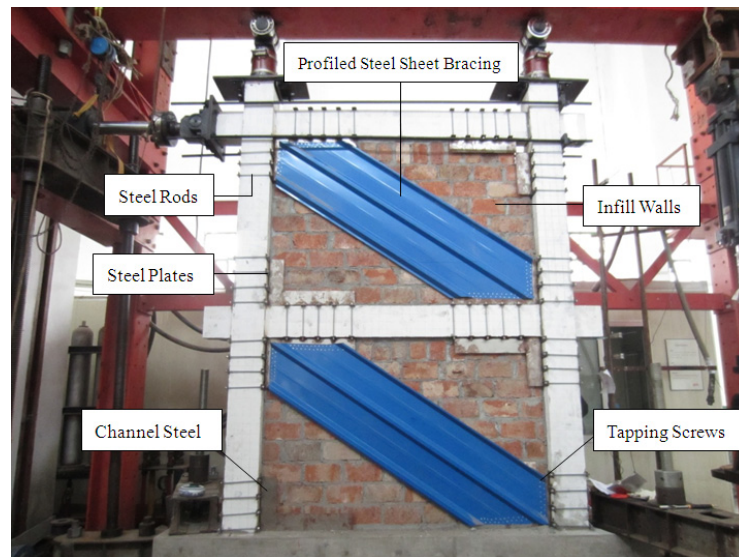


Fig. 3 Photograph of the layouts of Specimens KJ-2

Table 1 Properties of reinforcing bars

Type	Diameter (mm)	Yield strength f_y (MPa)	Ultimate strength f_u (MPa)	Elongation (%)
Longitudinal bars	10	382.11	579.37	25.0
Transversal ties	8	390.36	596.63	26.3

2.2 Materials

When casting the frames, six $150 \times 150 \times 150$ mm concrete cubes were made in the same condition. The strength of concrete cubes was tested after curing 28-day, according to Chinese Standard Design Code (2010). The average compressive strength of concrete cubes was 38.23 MPa. The yield strength of longitudinal bars and transversal ties were 382.11 MPa and 390.36 MPa, while the ultimate strength were 579.37 MPa and 596.63 MPa, respectively. The properties of reinforcing bars are summarized in Table 1.

The size of the fired common brick was $240 \times 115 \times 53$ mm. According to size effect of the frame, the fired common brick was constructed in vertical. In other words, the height of fired common brick was 115 mm, and the thickness of infill walls was 53 mm. The average compress-

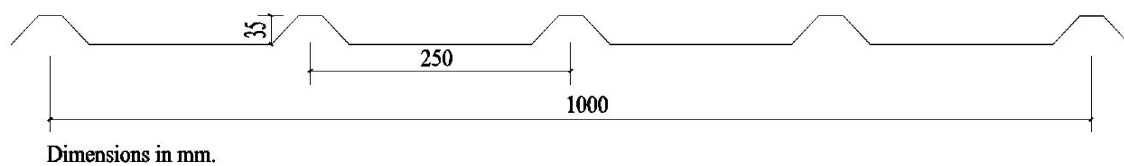


Fig. 4 Cross section dimensions of profiled steel sheeting

Table 2 Properties of concrete, fired common brick and profiled steel sheeting

Component	Concrete compressive strength $f_{cu,k}$ (MPa)	Fired common brick compressive strength f (MPa)	Yield strength f_y (MPa)	Ultimate strength f_u (MPa)	Elongation (%)
Concrete	38.23	—	—	—	—
Fired common brick	—	22.62	—	—	—
Profiled steel sheeting	—	—	264.15	365.04	14.2

sive strength of fired common brick was 22.62 MPa, which was measured as per Chinese Standard (2003). The portion of cement mortar was 1:3 (cement: sand). The profiled steel sheeting of YX35-250-1000 with 0.4 mm thickness was used for frame strengthening. The yield strength of profiled steel sheeting was 264.15 MPa. The ultimate strength of profiled steel sheeting was 365.04 MPa. Cross section dimensions of profiled steel sheeting are shown in Fig. 4. The properties of concrete, fired common brick and profiled steel sheeting are listed in Table 2.

2.3 Test setup and loading program

Test setup is shown in Fig. 5. Instrumentation plan is shown in Fig. 6. Strain and deformation were measured through the strain gauge and displacement transducers, respectively. Furthermore, the data of strain and deformation was collected by static collection device. Strain gauge was used to measure the changes of strain, which was attached to the longitudinal bars and transversal ties. In the light of the change of strain to infer when the steel bars yielded. Hydraulic jack offered the low-cyclic lateral load, which was applied to specimens at the beam end. On the top of two

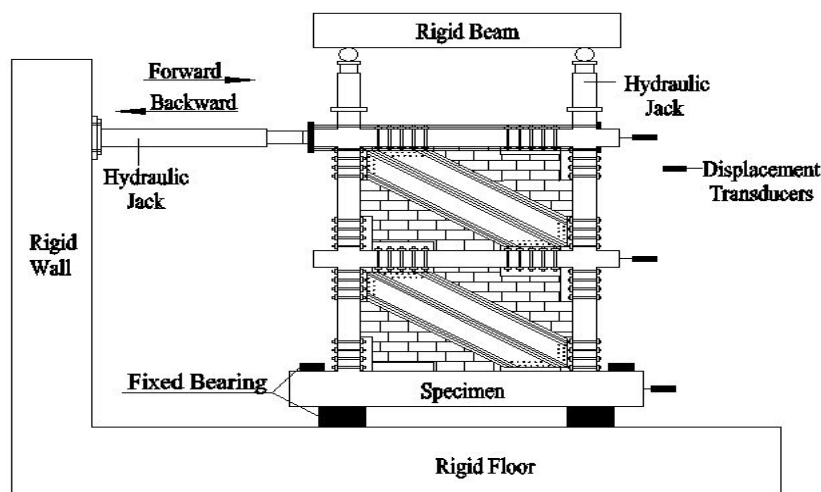


Fig. 5 Test setup of the specimen

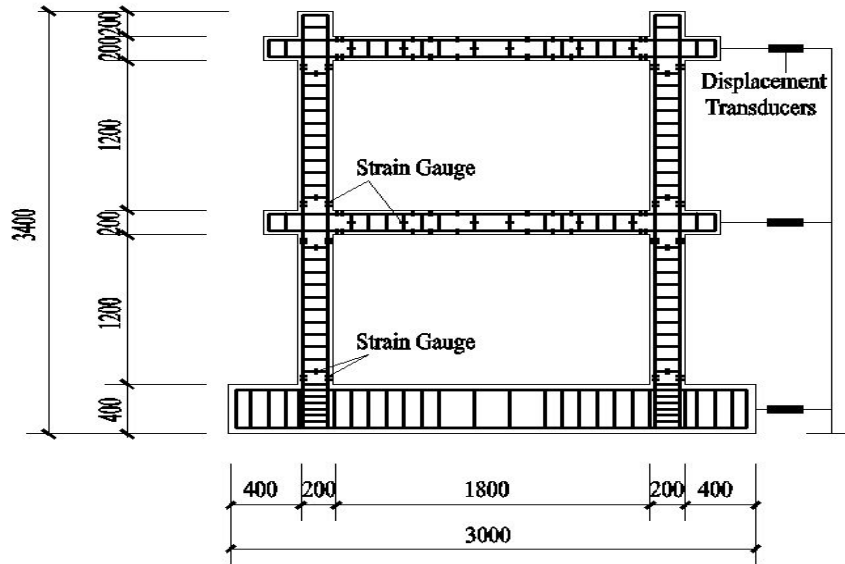


Fig. 6 Instrumentation plan

columns, hydraulic jacks were fixed by the rigid beam, which provided the vertical force (200 kN). When the frame deflected, the rollers between hydraulic jacks and rigid beam moved with the frame. The vertical force and the column kept the same vertical plane. It would not produce additional bending moments to affect the structural performance.

Loading program of two specimens adopted force control first and controlled displacement later. At the beginning, the lateral load was increased by 10 kN in each cycle. The measured strain in longitudinal bars reached $2052 \mu\epsilon$ at the bottom of left column, which was the theoretical yielding value. When longitudinal bars yielded, loading modes changed to the controlled displacement and recorded the displacement value Δ_y (yielded displacement). The controlled displacement was increased by the displacement value Δ_y of integer at each cycle. Each cycle repeated three times until the frame was destroyed or the lateral load fell below 85% of the ultimate load, tests were terminated. This lateral load was the failure load. The ultimate load was the maximum value of the lateral load in loading. Loading program of specimen KJ-2 is shown in Fig. 7.

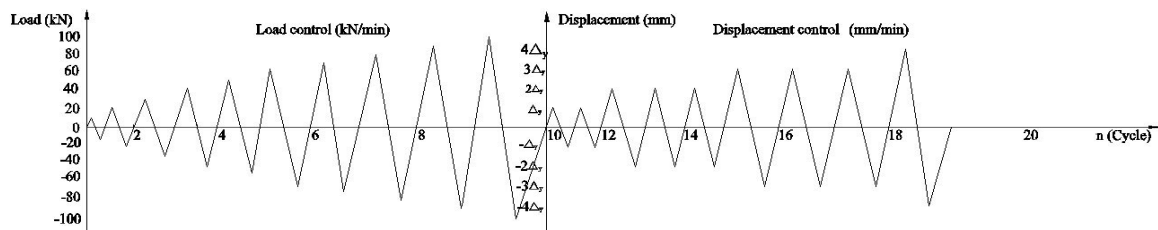


Fig. 7 Loading program of KJ-2

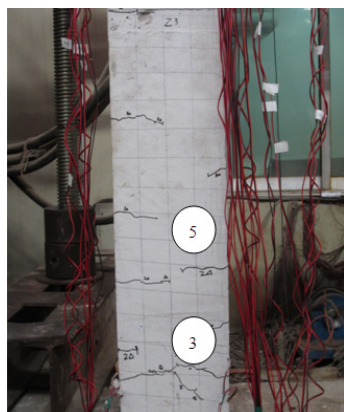
3. Experimental results and discussion

3.1 Failure mechanism and hysteretic curves

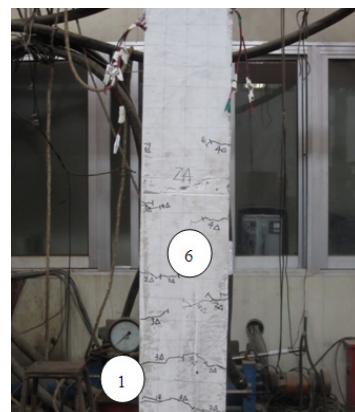
The partial cracks in KJ-1 are shown in Fig. 8. Cracks have not appeared until 10 kN, which indicated that KJ-1 was still in the elastic stage. When the lateral load reached 11 kN, the first crack formed at right column bottom (Fig. 8(c) No. 1). When the lateral load reached 28 kN, some vertical cracks appeared on the beam end (Fig. 8(a) No. 2). Two cracks formed at the bottom of left columns at 30 kN (Fig. 8(b) No. 3). When the controlled displacement reached $\pm \Delta_y$, the original cracks on the left column grew continuously and new vertical cracks formed on the beam end (Fig. 8(a) No. 4). Horizontal cracks formed from the left column bottom 20 cm, 30 cm and 35 cm (Fig. 8(b) No. 5) and diagonal crack from beam end 55 cm (Fig. 8(a) No. 5) when the controlled displacement was $\pm 2\Delta_y$. Cracks grew from the right column bottom 40 cm, 50 cm and 65 cm (Fig. 8(c) No. 6) when the controlled displacement was $\pm 3\Delta_y$. When the controlled displacement reached $\pm 4\Delta_y$, new diagonal crack formed on the beam end (Fig. 8(a) No. 7) and the original crack from the right column bottom 40 cm developed further.



(a) Cracks on the beam



(b) Cracks at the left column



(c) Cracks at the right column

Fig. 8 Partial cracks in KJ-1

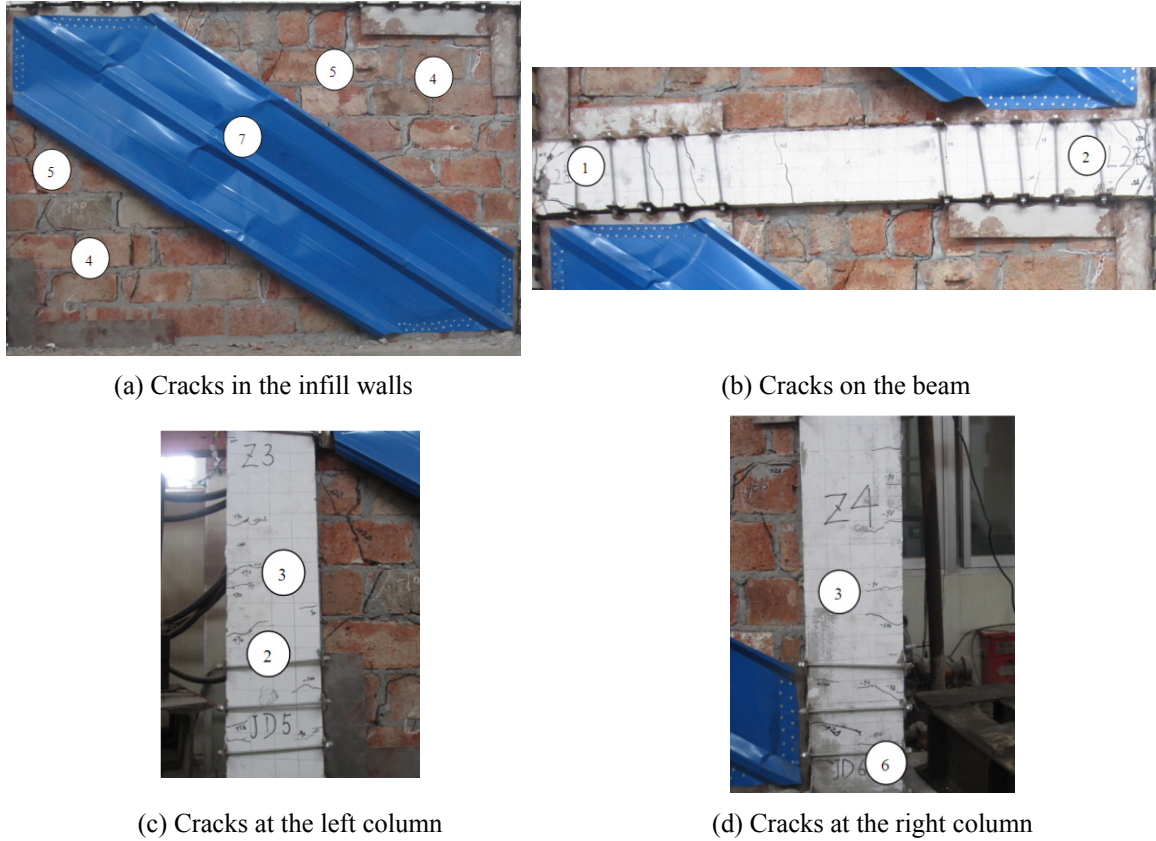


Fig. 9 Partial cracks in KJ-2

The partial cracks in KJ-2 and deformation of profiled steel sheet bracing are shown in Fig. 9. Cracking load was 37 kN, which formed on the beam end (Fig. 9(b) No. 1). When the lateral load reached 80 kN, new cracks formed from the right beam end 10 cm (Fig. 9(b) No. 2) and from the left column bottom 40 cm (Fig. 9(c) No. 2). Meanwhile profiled steel sheet bracing developed recoverable deformation. There were new cracks in the middle of both columns when the lateral load was 90 kN (Figs. 9(c) and (d) No. 3). Bottom left corner of profiled steel sheet bracing formed unrecoverable deformation. When the lateral load reached 100 kN, the longitudinal bars at the bottom of left column yielded. Bottom left corner and top right corner of infill walls formed cracks (Fig. 9(a) No. 4). The cracks developed along diagonal direction when the controlled displacement was $\pm \Delta_y$. When the controlled displacement reached $\pm 2\Delta_y$, new cracks (Fig. 9(a) No. 5) in the wall increased and profiled steel sheet bracing formed local buckling. When the controlled displacement reached $\pm 3\Delta_y$, parts of solder joints between channel steel and steel plates cracked gradually and broken brick of infill walls corners fell. When the controlled displacement reached $\pm 4\Delta_y$, the center of infill walls was out-of-plan. The right column bottom was crushed (Fig. 9(d) No. 6). The center of profiled steel sheet bracing buckled severely (Fig. 9(a) No. 7).

Hysteretic curves of test specimens are shown in Fig. 10. It can be seen from the figures that the curves were linear in the initial phase. The deformation of specimens can be recovered in the elastic stage. At this stage, lateral load of Specimen KJ-1 was from 0 kN to 15 kN, while the

lateral load of Specimen KJ-2 was from 0 kN to 45 kN. With the increase of loading, the cracks of concrete spread continually. At the same time, compressive strain of concrete and tensile strain of steel bar increased constantly. As can be seen from Fig. 10(a), yield load of Specimen KJ-1 was 32.74 kN in forward loading. In backward loading, the yield load was 30.13 kN. Based on the results presented in Fig. 10(b), yield load of Specimen KJ-2 was 99.77 kN in forward loading, while the yield load was 90.64 kN in backward loading. In the controlled displacement, the increasing area of hysteretic loop showed that energy dissipation enhanced gradually. Curve slope of the first cycle was larger than that of the second and third cycle under the same loading level. This phenomenon indicated that stiffness of test specimen degenerated under low-cyclic lateral loading. The ultimate loads of Specimen KJ-1 were 43.69 kN and 40.14 kN, respectively. The ultimate loads of Specimen KJ-2 were 142.2 kN and 122.46 kN, respectively. In the final phase, cracks in concrete and infill walls grew obviously and hysteretic loop appeared pinch effect in some extent. Stiffness degeneration of specimens was serious.

Yield load and ultimate load are presented in Table 3. The results showed that reinforcement method of Specimen KJ-2 had a significant strengthening effect in the test. Yield load and ultimate load of Specimen KJ-2 was 3 times greater than that of Specimen KJ-1. In addition, after the failure of infill walls and the buckling of profiled steel sheet bracing, a great of portion of lateral load was transferred to the columns. As a result, the strength of Specimen KJ-2 showed some decrease.

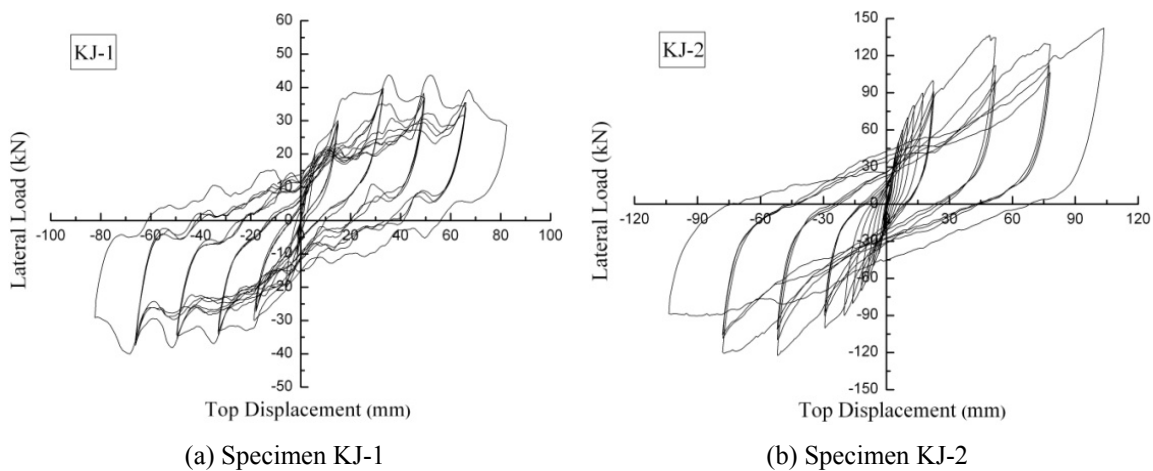


Fig. 10 Hysteretic curves of specimens

Table 3 Comparisons of yield load and ultimate load

Specimens	Forward				Backward			
	Yield load (kN)	Ultimate load (kN)	Ratio ^a	Ratio ^b	Yield load (kN)	Ultimate load (kN)	Ratio ^a	Ratio ^b
KJ-1	32.74	43.69	1.00	1.00	30.13	40.14	1.00	1.00
KJ-2	99.77	142.2	3.05	3.25	90.64	122.46	3.0	3.06

^a Ratio: Yield load of Specimen KJ-2/ Yield load of Specimen KJ-1;

^b Ratio: Ultimate load of Specimen KJ-2/ Ultimate load of Specimen KJ-1

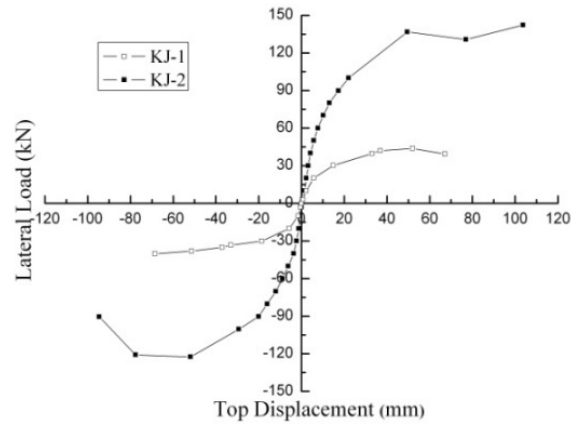


Fig. 11 Envelope curves of specimens

Table 4 Comparisons of yield displacement, failure displacement and ductility coefficient

Specimens	Forward			Backward		
	Yield displacement (mm)	Failure displacement (mm)	Ductility coefficient	Yield displacement (mm)	Failure displacement (mm)	Ductility coefficient
KJ-1	19.8	67.2	3.39	18.75	68.5	3.65
KJ-2	25.73	103.69	4.03	20.43	94.61	4.63

3.2 Envelope curves of specimens

The load-displacement envelope curves of test specimens are shown in Fig. 11. It can be seen from the figures that envelope curves of two specimens were almost the same within the scope from 0 kN to 15 kN. The curve of Specimen KJ-2 was higher than that of Specimen KJ-1 after 15 kN. This was attributed to the added profiled steel sheet bracing and infill walls, which increased strength of Specimen KJ-2. With the increase of the load, the envelope curves of two specimens enhanced gradually. However, the envelope curves of Specimen KJ-1 increased slower than that of Specimen KJ-2. As can be seen from Fig. 11, Specimen KJ-1 reached failure load earlier.

Yield displacement, failure displacement and ductility coefficient are presented in Table 4. Zhu (1989) defined the ductility coefficient μ , which expressed the ductility of structure and could be calculated by Eq. (1).

$$\mu = \frac{\Delta_u}{\Delta_y} \quad (1)$$

Where Δ_y is the yield displacement, Δ_u is the failure displacement.

The ductility of structure reflects the ability of deformation and absorbing seismic energy. As can be seen from the table that the yield displacement and failure displacement of KJ-2 were higher than KJ-1. This indicated that the profiled steel sheet bracing and infill walls increased the strength of RC frame. As can be seen from Table 3, yield load and ultimate load of Specimen KJ-2 was 3 times greater than that of Specimen KJ-1. Furthermore, the profiled steel sheet bracing and

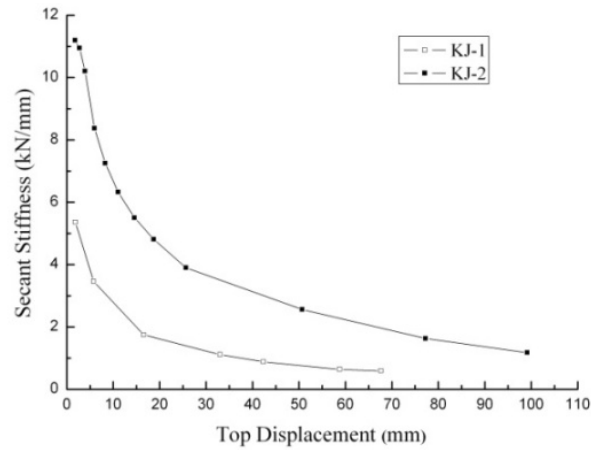


Fig. 12 Stiffness degradation curves of specimens

infill walls increased the stiffness of the frame. On the basis of these results, ductility coefficient of KJ-2 was 1.18 times greater than that of KJ-1. This demonstrated that the ability of deformation and absorbing energy of KJ-2 had an advantage over KJ-1.

3.3 Stiffness degradation curves of specimens

Secant stiffness K_i is introduced as per Chinese Standard (1997), which represents the stiffness of specimens and can be calculated by Eq. (2).

$$K_i = \frac{|+ F_i| + |- F_i|}{|+ X_i| + |- X_i|} \tag{2}$$

Where F_i is the peak load of each cycle, X_i is the peak displacement of each cycle, “+” is forward loading, and “-” is backward loading.

Stiffness degradation curves of test specimens are shown in Fig. 12. Stiffness of two specimens declined during the loading. Specimen KJ-1 showed a clear decline from 5.36 kN/mm to 2.6 kN/mm. In addition, Specimen KJ-2 declined from 11.19 kN/mm to 5.5 kN/mm. The stiffness decrement percentages of the specimens are 51.49% and 50.85%, respectively. After yielding, stiffness curves of two specimens declined slowly. The stiffness of specimen KJ-2 was higher than specimen KJ-1.

Table 5 Stiffness values at different stages

Specimens	Initial (kN/mm)	At failure load (kN/mm)	Ratio ^a	Ratio ^b
KJ-1	5.36	0.59	1.00	1.00
KJ-2	11.19	1.17	2.09	1.98

^a Ratio: Initial stiffness of Specimen KJ-2/ Initial stiffness of Specimen KJ-1;

^b Ratio: Stiffness of Specimen KJ-2/Stiffness of Specimen KJ-1, at failure load

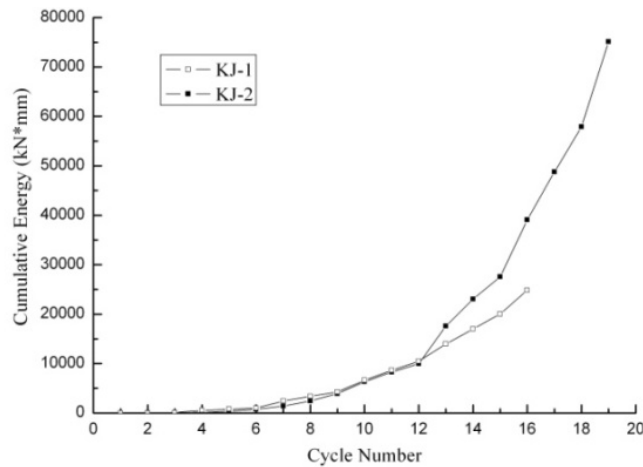


Fig. 13 Energy dissipation of specimens

Stiffness values at different stages are presented in Table 5. It can be seen from the table that the initial stiffness of Specimen KJ-2 was 2 times greater than that of specimen KJ-1. At failure load, the initial stiffness of Specimen KJ-2 was 1.9 times greater than that of Specimen KJ-1. It demonstrated that profiled steel sheet bracing and infill walls increased the stiffness of KJ-2 obviously.

3.4 Energy dissipation capacities

The energy dissipation can be illuminated by the area inside the hysteresis loop of each cycle, which reflects energy dissipation of structure. Fig. 13 depicts the variation of cumulative energy as a function of cycle number. The higher value of cumulative energy indicated the stronger ability of seismic energy absorption. Within the scope from 1 to 12 cycle, the curves were similar and almost coincident. Cracks distribution in KJ-1 were at the right column bottom 40 cm, 50 cm and 65 cm (Fig. 8(c) No. 6) and KJ-1 has reached ultimate load in Fig. 11. Columns bore the main lateral load, which dissipated a great deal input energy. At this time, cracks in KJ-2 distributed in bottom left corner and top right corner of infill walls (Fig. 9(a) No. 4) and developed along diagonal direction. Infill walls bore the main lateral load and dissipated plenty of energy. Energy dissipation of Specimen KJ-2 had an obvious promotion after 12 cycles. This promotion of cumulative energy indicated the good coordination of profiled steel sheet bracing and infill walls in Specimen KJ-2. Under low-cyclic loading, profiled steel sheet bracing and infill walls acted as the members of tensile resistance and compressive resistance, respectively. With new cracks (Fig. 9(a) No. 5) in the wall developed and profiled steel sheet bracing buckled, cumulative energy continued to rise. Until the right column bottom was crushed (Fig. 9(d) No. 6), cumulative energy reached the maximum value.

4. Conclusions

One-bay, two-story, 1/3 scale two specimens have been investigated in the experiment.

Furthermore, the results of two specimens have been compared in the light of test data. The conclusions are as follows:

- The ultimate load of Specimen KJ-2 was 225% higher than that of Specimen KJ-1. This demonstrated that there was a significant effect on reinforcing Specimen KJ-2 with profiled steel sheet bracing and infill walls. The strength of Specimen KJ-2 has been improved greatly.
- Comparing with crack distribution of Specimen KJ-1, some cracks in Specimen KJ-2 distributed in infill walls. In addition, deformation of profiled steel sheet bracing has been described. This demonstrated that strengthening member shared the lateral load effectively.
- As can be seen from Fig. 11, the stiffness of Specimen KJ-2 was approximately 2 times than that of Specimen KJ-1. This showed that profiled steel sheet bracing and infill walls took an active role in loading.
- Energy dissipation of KJ-2 had a significant increase after 12 cycles. This indicated that Specimen KJ-2 was able to bear the lateral load effectively. Profiled steel sheet bracing and infill walls worked together to resist the lateral load. Seismic performance of RC frames has been improved.
- The advantages of profiled steel sheeting were light, low cast and saving steel. In terms of operating, it was convenient to connect. Based on the advantages, profiled steel sheeting had a wide application prospect in strengthening structures.

Acknowledgments

This work is supported by Key Technology R&D Program of Jiangsu Province (No: BE2011791).

References

- Ahmed, E. and Badaruzzaman, W.H.W. (2013), "Vibration performance of profiled steel sheet dry board composite floor panel", *KSCE J. Civil Eng.*, **17**(1), 133-138.
- Altin, S., Anil, Ö., Kara, M.E. and Kaya, M. (2008), "An experimental study on two different strengthening techniques for RC frames", *J. Compos. Part B*, **39**(4), 680-693.
- Badoux, M. and Jirsa, J.O. (1990), "Steel bracing of RC frames for seismic retrofitting", *J. Struct. Eng.*, **116**(1), 55-74.
- Bush, T.D., Jones, E.A. and Jirsa, J.O. (1991), "Behavior of RC frame strengthened using structural steel bracing", *J. Struct. Eng.*, **117**(4), 1115-1126.
- Chen, S.M. (2002), "Study of load-carrying capacities of 3W-DECK composite slabs", *J. Build. Struct.*, **23**(3), 19-26.
- Design Code (1997), *Specifying of Testing Methods for Earthquake Resistant Building*, JGJ 101-96, Beijing, China.
- Design Code (2003), *Test Methods for Wall Bricks*, GB/T 2542-2003, Beijing, China.
- Design Code (2010), *Code for Design of Concrete Structures*, JB 50010-2010, Beijing, China.
- Erdem, I., Akyuz, U., Ersoy, U. and Ozcebe, G. (2006), "An experimental study on two different strengthening techniques for RC frames", *Eng. Struct.*, **28**(13), 1843-1851.
- Fell, B.V., Kanvinde, A.M., Deierlein, G.G. and Myers, A.T. (2009), "Experimental investigation of inelastic cyclic buckling and fracture of steel braces", *J. Struct. Eng.*, **135**(1), 19-32.
- Guo, R. and Zhao, S.W. (2012), "Experimental study on seismic performance of combination strengthening RC frame", *Earthq. Resist. Eng. Retrofit.*, **34**(5), 34-39.

- Li, Y.S., Shan, W., Huang, Z.b., Ge, B.D. and Wu, Y. (2008), "Experimental study on mechanical behavior of profiled steel sheet-bamboo plywood composite slabs", *J. Build. Struct.*, **29**(1), 96-102.
- Maheri, M.R. and Hadjipour, A. (2003), "Experimental investigation and design of steel brace connection to RC frame", *Eng. Struct.*, **25**(13), 1707-1714.
- Nie, J.G. and Yi, W.H. (2005), "Bearing capacity and calculation method of profiled steel sheeting-concrete composite slabs", *Build. Struct.*, **35**(1), 49-52.
- Tzaros, K.A., Mistakidis, E.S., and Perdikaris, P.C. (2010), "A numerical model based on nonconvex-nonsmooth optimization for the simulation of bending tests on composite slabs with profiled steel sheeting", *Eng. Struct.*, **32**(3), 843-853.
- Wang, S.G., Lan, Z.J. and Lan, Z.J. (1998), "Behavior of reinforced concrete frame with energy-dissipation bracings under reversed cyclic loads", *Earthq. Eng. Eng. Vib.*, **18**(3), 124-130.
- Yu, H.F. (2009), "Aseismic performance of welded I-section steel bracings and concentrically braced steel frames", Ph.D. Dissertation, Harbin Institute of Technology, Harbin, China.
- Zhao, B.C., Yu, A.L., Jiang, S.C. and Wang, J.L. (2013), "Experimental investigation of Y-eccentrically steel braced RC frames energy-dissipation", *Earthq. Eng. Eng. Vib.*, **33**(1), 47-53.
- Zhu, B.L. (1989), *Structural Seismic Test*, Seismological Press, Beijing, China.
- Zhu, J.T., Wang, X.L., Xu, Z.D. and Weng, C.H. (2011), "Experimental study on seismic behavior of RC frames strengthened with CFRP sheets", *Compos. Struct.*, **93**(6), 1595-1603.

CC